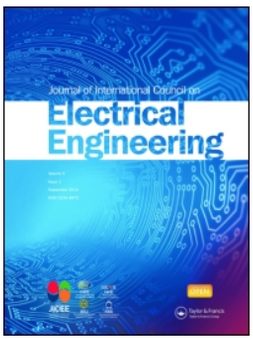

Journal of International Council on Electrical Engineering

ISSN: (Print) 2234-8972 (Online) Journal homepage: https://www.tandfonline.com/loi/tjee20

Development of dynamic simulator of alkaline water electrolyzer for optimizing renewable energy systems

H. Kojima, T. Matsuda, H. Matsumoto & T. Tsujimura

To cite this article: H. Kojima, T. Matsuda, H. Matsumoto & T. Tsujimura (2018) Development of dynamic simulator of alkaline water electrolyzer for optimizing renewable energy systems, Journal of International Council on Electrical Engineering, 8:1, 19-24, DOI: 10.1080/22348972.2018.1436931

To link to this article: https://doi.org/10.1080/22348972.2018.1436931

Published online: 19 Feb 2018.

JOURNAL OF INTERNATIONAL COUNCIL ON ELECTRICAL ENGINEERING
2018, VOL. 8, NO. 1, 19–24
https://doi.org/10.1080/22348972.2018.1436931

Taylor & Francis
Taylor & Francis Group

Development of dynamic simulator of alkaline water electrolyzer for optimizing renewable energy systems

H. Kojima[a], T. Matsuda[b], H. Matsumoto[a] and T. Tsujimura[a]

[a]Renewable Energy Research Center, National Institute of Advanced Industrial Science and Technology (AIST), Koriyama, Japan; [b]Department of Materials Science and Engineering, Graduate School of Engineering, Tokyo Denki University, Tokyo, Japan

ABSTRACT

In order to analyse dynamic behaviours of hydrogen production by alkaline water electrolysis against fluctuating electric power, we developed a large-scale electrolyzer simulator. The measurement data of a 150-kW alkaline water electrolyzer were used in the development of the simulator model. In this study, first, model constants relevant to heat balance in the system were determined based on experimental data obtained by the operation of a 150-kW electrolyzer, in order to simulate the hydrogen generation process over an extensive duration. The results showed that the model can predict the temperature over a period of 24 h. Next, the prediction of temperature and efficiency for different scales of electrolyzers was conducted using the developed simulator to assess the behaviour of various large-scale electrolyzers in practical use. In a large-scale electrolyzer, temperature change due to heat transfer to ambient air reduces; thus, such electrolyzers have an advantage in terms of energy-conversion efficiency. Furthermore, the performance of one large electrolyzer (5 MW) and two small electrolyzers (1 MW each) was predicted and compared. The large electrolyzer had an advantage after its temperature increased because the moderate electrolyzer temperature and low current density could be achieved concurrently owing to a slower cooling speed.

ARTICLE HISTORY
Received 3 December 2017
Accepted 26 January 2018

KEYWORDS
Alkaline water electrolyzer; renewable electricity; hydrogen production; renewable energy system; dynamic simulator; systems modelling

1. Introduction

The Fukushima Renewable Energy Institute of AIST (FREA), Japan, has the world's largest class hydrogen energy carrier production, storage and utilization system. While the system was in operation, measurements were conducted to assess the system's performance and for the purpose of suggesting new systems and control methods. In order to develop an energy-efficient system for practical applications using renewable electricity, the analysis of dynamic behaviours against fluctuating electric power generated by photovoltaic cells and wind turbines is essential. In this system, electricity is converted to hydrogen energy via water electrolysis. Then, methylcyclohexane, which is an organic chemical hydride, is produced by hydrogenation reactors for energy storage. In electrolysis, the voltage of the electrolytic cell, which should be small to ensure higher energy efficiency, changes in relation to the current density and temperature. According to the measurement results, current density and temperature change dynamically depending on the pattern of renewable electric power [1]; therefore, an analysis with consideration to the unsteady behaviour of the electrolyzer is essential.

Such an analysis can be conducted using a dynamic simulator. For example, Ulleberg developed an electrolyzer simulation model, which includes an electrochemical and a thermal model for energy system simulation [2]. Diéguez et al. analysed and modelled the thermal behaviour of an electrolyzer [3]. Authors have also developed a dynamic electrolyzer simulator based on experimental data obtained during the operation of a 150-kW class electrolyzer, whose pressure in tanks, hydrogen flow-rate change, oxygen concentration in hydrogen and the unsteady change of voltage and temperature were modelled [4]. Since electrolyzer predictions over the period of a week, month or year are important because of various scales of fluctuating input power patterns, these simulators require having the ability to predict temperature change over a long period of time.

In this study, model constants in the simulator were first determined for long-term operation (>24 h) in order to investigate the hydrogen-production performance

CONTACT H. Kojima hirokazu-kojima@aist.go.jp

of a practical scale electrolyzer. Then, the dynamic behaviours of larger scale electrolyzers were examined over the period of a few days, using the developed simulator. We also performed an energy-efficiency comparison of one large and two small electrolyzers.

2. Calculation models and methods

A numerical simulator of a large-scale alkaline water electrolyzer was developed in order to estimate the performance of hydrogen production using renewable electricity. The base model used in the simulator was developed earlier [4]. In this study, the temperature-estimation model parameters were modified to accurately predict the temperature increase and decrease processes.

2.1. 150-kW alkaline water electrolyzer

An alkaline water electrolyzer was installed in the hydrogen energy production and utilization system as a hydrogen generator that uses reproduced renewable electricity. The simulator model was developed based on this electrolyzer and the schematic illustration is shown in Figure 1. The apparatus mainly constituted power sources, two sets of electrolysis cell stacks with $n_{\mathrm{cell}} = 41$ cells, a cathode tank, an anode tank and an electrolyte circulation pump. The power sources could supply a total of up to 160 kW of DC electricity to the electrolysis cell stacks. An electrode in the stacks had a cross-sectional area of 0.25 m^2 and the rated current was 1000 A, which amounts to 4000 $\mathrm{A/m}^2$ of current density. The electrolyte was approximately 30 wt% KOH, which was pumped from the tanks into the cell stacks. The flow rates of electrolyte supplied to the cell stacks' cathode and anode sides were adjusted to 1.5 m^3/h using valves. The mixture of electrolyte and generated gas flowed into the tanks and the liquid and gas phases were separated. Mist in gas coming from the tank was removed via a mist trap; water vapour at high temperature was condensed in a heat exchanger with cooling water, at room temperature. After passing through a flow-rate meter and a pressure sensor, the hydrogen from the cathode tank was sent to the hydrogenation reactors; oxygen from the anode tank was released to the atmosphere. At an input power of 150 kW and temperature of 80 °C, the rated hydrogen flow rate was 34 Nm^3/h.

2.2. Electrolysis cell and thermal model

Electrolysis cell characteristics were modelled considering the equilibrium voltage for water electrolysis, v_{eq}, resistance overvoltage, v_{r} and activation overvoltage, v_{a},

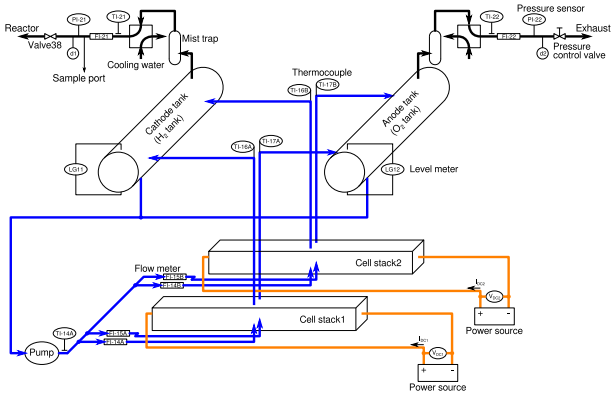

Figure 1. Schematic illustration of the 150-kW alkaline water electrolyzer installed in FREA.

based on the fundamental relations in water electrolysis [5]. The temperature dependences of overvoltage were considered via first-order approximation. The cell voltage, v_{cell}, is expressed against current density, i, and temperature, T, as follows:

$$v_{\mathrm{cell}} = v_{\mathrm{eq}}(T) + v_{\mathrm{r}}(i,T) + v_{\mathrm{a}}(i,T), \tag{1}$$

$$v_{\mathrm{eq}}(T) = \frac{\Delta G(T)}{nF}, \tag{2}$$

$$v_{\mathrm{r}}(i,T) = \left(\frac{d}{\sigma(T)} + R\right) Ai, \tag{3}$$

$$\sigma(T) = \sigma_0 \{1 + k_\sigma (T - T_0)\}, \tag{4}$$

$$v_{\mathrm{a}}(i,T) = k_{\mathrm{a}} \{1 + k_{\mathrm{Ta}}(T - T_0)\} \ln \frac{i}{i_0}, \tag{5}$$

where ΔG is the difference of Gibbs free energy of the water electrolysis reaction. In this reaction, $n = 2$, F is the Faraday constant, A is the area of an electrode, and T_0 (=25 °C) is the reference temperature; d/σ_0, R, k_σ, k_{a}, k_{Ta} and i_0 are model constants.

To determine the six model constants, a 150-kW electrolyzer was operated under various current inputs over a few hours. The instantaneous data points of current density i, cell voltage V_{cell} and temperature T, were distributed to blocks with 50 $\mathrm{A/m}^2$ and 5 °C intervals. In other words, time-series data were mapped on I–V curves. Then, the least squares method was used for predicting the I–V curve of the experimental data, by using Equation (1). The results are shown in Figure 2. The lines in the figure are plots of the estimated cell voltage, V_{cell}, against current density, i, for temperature values of $T = 20, 30, 40, 50, 60, 70$ and 80 °C. The dots in the figure represent the experimental data points. Note that the temperature values in the experiment were variable and are therefore not equal to those of the estimated curves in this graph. In other words, the dots are not necessarily on the lines only. For a wide range of temperature, from 20

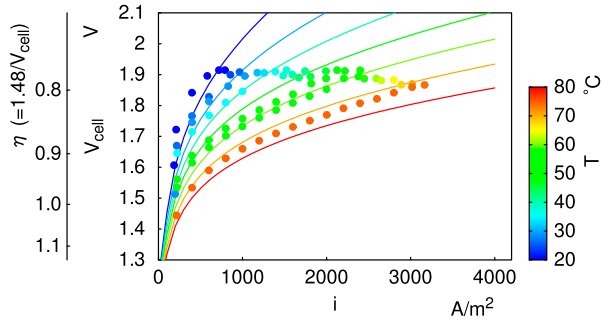

Figure 2. I–V curves of the used electrolytic cell. Dots represent measured values and lines represent estimated values.

to 80 °C, the cell model could predict the cell voltage; this is quite important in terms of electrolyzer performance.

In the dynamic simulator, temperature estimation is important because cell voltage varies with temperature, as shown in Figure 2. Thermal flow and heat capacity in this model were considered to predict the temporal change of temperature in the electrolyzer. A schematic illustration of the thermal flow considered in the model is shown in Figure 3. When input electric power is converted to hydrogen energy, heat is produced due to energy loss in the reaction, which in turn increases the electrolyzer's temperature. In an electrolyzer with high temperature, there are some release paths for thermal energy. High-temperature hydrogen, oxygen and water vapour bring energy out of the electrolyzer; the latent heat of water evaporation is not negligible. Pure water is supplied when the water level in the tank decreases due to water consumption by the reaction. Electrolyzer temperature decreases when low-temperature water and high-temperature electrolyte mix. Depending on the temperature difference, heat flows to ambient air according to Newton's law of cooling as expressed by:

$$\dot{Q}_c = h(T - T_{amb})A_s, \tag{6}$$

where h is the heat-transfer coefficient, T_{amb} is the ambient air temperature and A_s is the sum of the electrolyzer system's surface area.

In addition to the energy flow around the electrolyzer, the electrolyzer's heat capacity is considered when calculating temperature. To simplify the calculation, gross heat capacity is determined based on the mass of the electrolyte and the mass of structural materials such as the tank, pipe and electrodes, which is represented by the unknown model parameter m.

2.3. Modelling of large-scale electrolyzers

The electrolyzer simulator model described above was developed based on an actual 150-kW system. Since

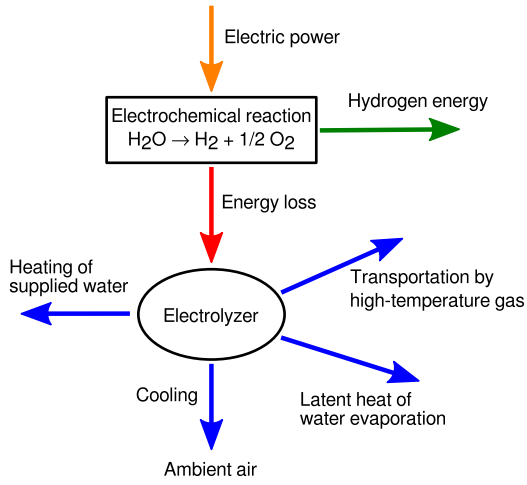

Figure 3. Energy-flow diagram of the electrolyzer simulation model.

larger-scale electrolyzers are expected to be combined with megawatt solar and wind farms, the ability to make predictions for electrolyzers of various scales is required. The model that was validated by the operation data of a 150-kW electrolyzer is discussed first. Then, model parameters for large-scale electrolyzers are discussed.

For larger-scale electrolyzers, rated powers of 1 and 5 MW were considered, and the area of electrodes was proportionally increased to 1.67 and 8.33 m^2, respectively, while maintaining the number of cells as 41. Since the hydrogen and oxygen production rates increase almost proportionally to input power, the electrolyte flow rate and tank volume should also be increased proportionally. In this case, the surface area of the electrolyzer system is proportional to the two-thirds power of the tank volume, under the assumption that the electrolyzer aspect ratio is the same. The cell characteristics shown in Figure 2 are assumed as applicable to all electrolyzers; the heat-transfer coefficient, h, is assumed to be the same.

3. Results and discussion

3.1. Model parameter optimization

The developed model has several model constants. Some of them can be determined from the specification of the system; others should be determined based on measured data. Six parameters relating to cell characteristics were determined by mapping the measured data on I–V curves as described above. The temperature of the electrolyzer is affected by unknown parameters such as the heat-transfer coefficient, h, and mass of materials, m.

In order to determine the unknown values, the 150-kW electrolyzer was operated for 24 h with fluctuating electricity input and with successive cooling periods during which there was no electricity input. The input

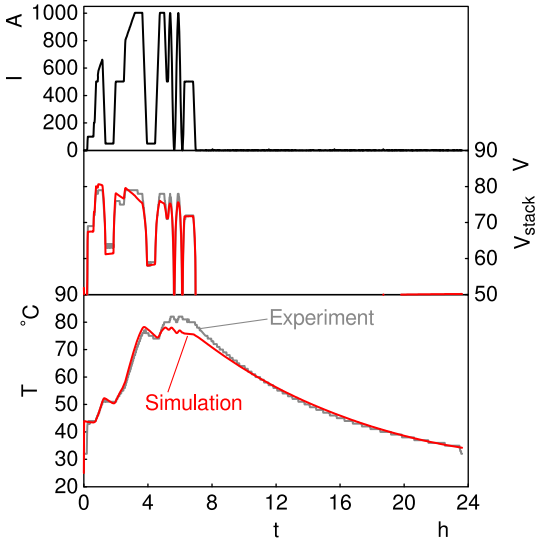

Figure 4. Temporal changes of stack voltage, V_{stack} and electrolyzer temperature, T, against input current, I, in the experiment and simulation for 24 h.

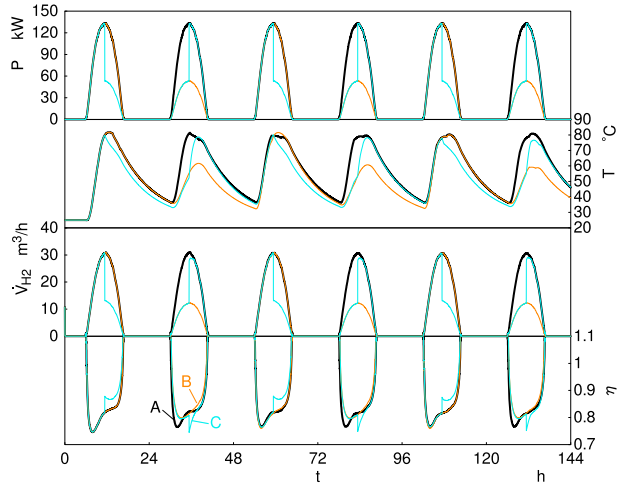

Figure 5. Predicted temporal changes of electrolyzer temperature, T, hydrogen flow rate, $\dot{V}_{H2}$ and electrolysis energy efficiency, η, against three patterns of input power, P, in the 150-kW electrolyzer.

current, I, stack voltage, V_{stack} and temperature, T, are plotted against time after the start of operation t in Figure 4. After the current input started, the value of V_{stack} changed in relation to the fluctuation of I; T increased gradually over time. At $t = 2$ and 4 h, T slightly decreased because the heat loss exceeded heat production due to a reaction caused by the low value of I. After $t = 7$ h, T decreased monotonically since there was no heat produced by the reaction. Parameters h and m were determined using the least squares method so that the simulation could predict the temperature profile obtained via the experiment. The values of $h = 5.5\,\mathrm{W/(m^2 \cdot K)}$ and $m = 2300$ kg were obtained as results. V_{stack} and T, which were calculated in the simulation using the parameters, h and m, are also shown in Figure 4. Despite the slight difference in the duration of high temperature, both heating and cooling processes in the simulation agree well with the experiment. This shows that the developed model can predict temperature change over a whole day.

3.2. Effect of input electric-power patterns

Using the developed simulator, which utilizes the model constants determined in the above discussion, hydrogen production performance was estimated for three simplified patterns, which reproduced PV power generation. A power pattern that was generated by 250-kW PV cells in FREA, on 10 October 2015, which was a very clear and sunny day, was taken as the base pattern. The measured power profile, P_{meas}, was adjusted to 150-kW scale by multiplying 0.6; the base pattern on 10 October was repeated six times to produce pattern A, which is an ideal power pattern comprising successive sunny days. The power profile is shown in Figure 5. For pattern B, the power was decreased to 40% of A in the 2nd, 4th and 6th day, which reproduced a profile of rotating sunny and cloudy days. In pattern C, the timing of sunny and cloudy conditions was shifted by 12 h in comparison to pattern B, where the power pattern changed at noon. Such simple patterns are useful in the fundamental investigation of the electrolyzer's dynamic; however, the ones mentioned above were pseudo-patterns, which do not necessarily reproduce the actual patterns of renewable electricity.

Simulation was conducted for patterns A, B and C and the results for temperature, T, hydrogen flow rate, $\dot{V}_{H2}$ and energy efficiency, η, are shown in Figure 5. Here, η is derived by assuming that current efficiency is unity such as:

$$\eta = \frac{1.48 \times n_{cell}}{V_{stack}}. \tag{7}$$

For pattern A, T increases when P increases, and η reaches its minimum value before P reaches its maximum value at $t = 12$ h. Then, η increases owing to the increase of T; η is approximately 0.8 at the time when P is maximum. When P decreases, T also starts to decrease, while η increases further. This is because the current density reduces and its effect is more influential than the decrease of T.

For pattern B, P was 40% of that for pattern A in the second day; the change in T was slow and small, owing to the lower heat produced by the reaction. As a result, although the current density for pattern B was much lower than that for pattern A, η had almost the same value at the peak-P timing $t = 36$ h. T in pattern B was smaller than that in pattern A on the second day but almost the same on the third day; this indicates that the delay time

of temperature change in the 150-kW electrolyzer was shorter than 24 h. The previous day's operation history was not significant.

For pattern C, where power changed at the timing of peak power, η changed by more than 0.05 at the timing of the P change owing to the large increase or decrease of current density. On the second day, T was not sufficiently high before $t = 36$ h, because P was low. Then, η dropped to approximately 0.75 when the input power was suddenly increased. As a result, η in pattern C was clearly observed to be lower than that in pattern A.

3.3. Effect of electrolyzer scale

Simulations of 1 and 5 MW electrolyzers were performed to investigate performance with regard to larger-scale hydrogen production. Although the 150-kW electrolyzer model was based on an actual system, the two larger electrolyzers were not actual systems and were only considered for simulation purposes. In the simulation, the model constants were reasonably set, as described above. Input power was also increased proportionally with the electrolyzer scale.

Figure 6 shows the simulation results of temperature, T, and the change of efficiency, η, with time, during three successive sunny days. Electric power input, P, was set according to the electrolyzer scale (as shown in Figure 6). The initial temperature was 25 °C in all cases and the temperature rise processes were almost identical before peak and power input. After P started decreasing at $t = 12$ h, the decrease of T owing to heat transfer to ambient air was faster for the 150-kW electrolyzer than it was for the 1-MW and 5-MW electrolyzers. The amount of heat produced by the reaction was proportional to the input power; the amount of electrolyte and materials was proportional to the size of the apparatus; the time-scale for temperature increase was also the same in all the cases. On the other hand, since volume change causes the surface area of the apparatus to become large proportionally to the two-thirds power of the system volume, heat transfer due to cooling becomes relatively small in the large-scale electrolyzers. In the 5-MW electrolyzer, approximately 50 °C remains overnight and T reaches a high value earlier, which leads to higher efficiency during start up at approximately $t = 30$ h.

3.4. Combination of electrolyzers

According to the dynamics discussed above, the efficiency of electrolysis changes with time in relation to current density and temperature. If enough power is available

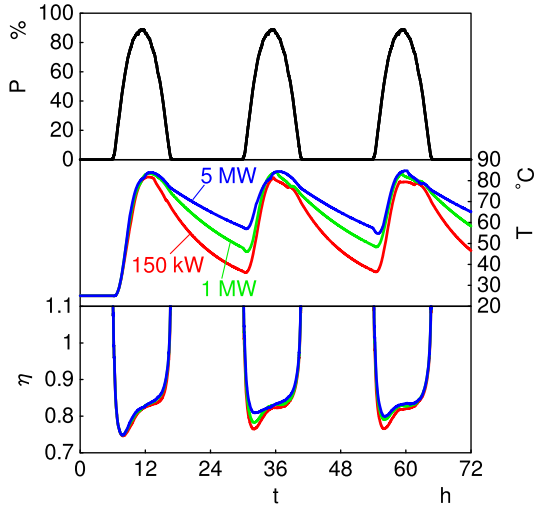

Figure 6. Predicted performance for three different scales of electrolyzers: 150 kW, 1 MW and 5 MW.

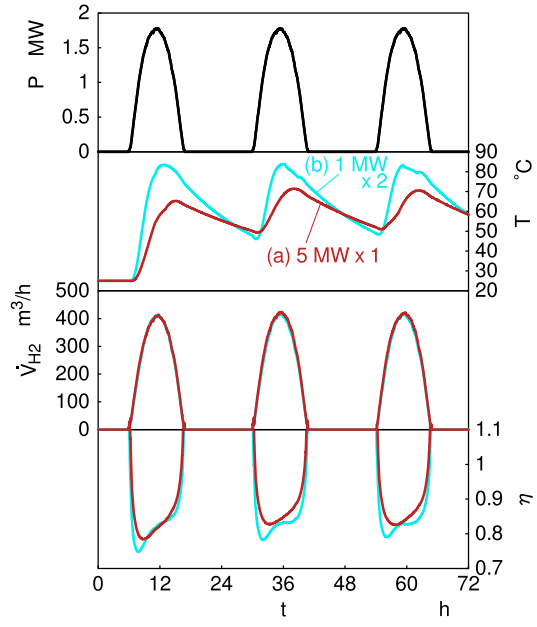

Figure 7. Performance predictions and comparison of a 5-MW electrolyzer and two 1-MW electrolyzers.

on a sunny day, a large-scale electrolyzer has the advantage of maintaining high efficiency because the cooling loss rate is relatively small. However, if the power input is low, a large electrolyzer is supposed to operate at low temperature, which results in low-efficiency operation. In this case, more efficient operation may be possible by using multiple small electrolyzers. In this study, two cases were investigated where the power input on a cloudy day was less than 2 MW: (a) one using a 5-MW electrolyzer and (b) the other using two 1-MW electrolyzers. A simulation was conducted for the 2-MW class power pattern, and the results are shown

in Figure 7. In the case of case (a), temperature did not increase sufficiently owing to the load being low compared with the scale of the apparatus. Nevertheless, the efficiency in this case was almost the same as that in case (b) because current density was lower in case (a). In the next day, at the beginning and end of the electrolysis process, T in case (a) was almost the same as that in case (b), owing to the dynamic behaviour of heat production and cooling. The efficiency in case (a) was always higher on the second and third days; therefore, the large-scale electrolyzer had an advantage in terms of energy efficiency when the power input was low. Since this is a simplified discussion, further investigation is required with regard to the consumed power of auxiliary machines, hydrogen impurity and strongly fluctuating power patterns.

4. Conclusions

A dynamic simulator of an alkaline water electrolyzer was developed on the basis of a 150-kW electrolyzer and its experimental data. The performance of hydrogen production with fluctuating power input and the scale effect were investigated.

Electrolysis cell characteristics were modelled using fundamental electrochemical relations. The temperature change was calculated using thermal flow processes. The abovementioned simulator model was successful in predicting temperature change over a 24-h period. The temperature increased and decreased repeatedly depending on the electric power input; this affected the hydrogen-production efficiency. On a cloudy day, temperature increase was suppressed and the current density was low. Further, the results showed that the efficiency was maintained, though the amount of hydrogen production being small.

A simulator was used for investigating the performance of a larger-scale combination of PV panels and electrolyzers. The temperature increase processes for 1-MW and 5-MW electrolyzers were almost identical. This was due to heat generated by a reaction, whose amount was proportional to the scale of the apparatus. On the other hand, the cooling speed decreases for a larger electrolyzer; therefore, on the next day, high-efficiency operation was realized during the start-up period. A larger electrolyzer also has an advantage in low-load operation owing to the moderate electrolyzer temperature and low current density being achieved concurrently.

Disclosure statement

No potential conflict of interest was reported by the authors.

Notes on contributors

H. Kojima is a researcher of National Institute of Advanced Industrial Science and Technology (AIST), Koriyama, Japan. He received his PhD in Energy Science from Kyoto University, Kyoto, Japan, in 2012. He joined AIST in 2012. His research interests are hydrogen energy carrier production/utilization systems and engine combustion.

T. Matsuda was born in Tokyo, Japan on 5 February 1995. He received his Bachelor's degree from the Department of Environmental Chemistry at the Tokyo Denki University, Tokyo, Japan, in 2017. He is now a graduate student at the Department of Materials Science and Engineering, Graduate School of Engineering, Tokyo Denki University, Tokyo, Japan. His research interests are hydrogen energy carrier production/utilization systems.

H. Matsumoto is a senior researcher of National Institute of Advanced Industrial Science and Technology (AIST), Koriyama, Japan. He received his Doctor of Engineering at Tokyo Institute of Technology (Tokyo Tech.), Tokyo, Japan in 1999. He was as an assistant professor (1999-2010) and an associate professor (2010-2015) in the Department of Chemical Engineering at Tokyo Tech. He works as a senior researcher in Renewable Energy Research Center (RENRC) at the Fukushima Renewable Energy Institute, AIST (FREA) since 2015, due to the personnel exchange program in faculty of engineering at Tokyo Tech. His research interests include modeling and simulation of reaction process for hydrogen energy carrier production/utilization, process intensification and chemical engineering application of intelligent systems technology.

T. Tsujimura is a team leader of National Institute of Advanced Industrial Science and Technology (AIST). He earned his Doctor of Engineering on hydrogen jet and combustion at Doshisha University, Japan. He joined the AIST from 2004 and had been involved in research on new fuels for engine combustion. He is currently working for renewable energy and hydrogen energy carrier.

References

[1] Kojima H, Matsumoto H, Tsujimura T. Development of large scale unified system for hydrogen energy carrier production and utilization: experimental analysis and systems modeling. Int J Hydrogen Energy. 2017;42:13444–13453.

[2] Ulleberg Ø. Modeling of advanced alkaline electrolyzers: a system simulation approach. Int J Hydrogen Energy. 2003;28:21–33.

[3] Diéguez PM, Ursúa A, Sanchis P, et al. Thermal performance of a commercial alkaline water electrolyzer: experimental study and mathematical modeling. Int J Hydrogen Energy. 2008;33:7338–7354.

[4] Kojima H, Matsumoto H, Tsujimura T. Modeling of 150kW class alkaline water electrolyzer for hydrogen production from renewable electricity. In: ICEE2016 Proceedings, ID:90490; 2016.

[5] Zeng K, Zhang D. Recent progress in alkaline water electrolysis for hydrogen production and applications. Prog Energy Combust Sci. 2010;36:307–326.